Study of the Kinetics of the Recrystallization of Cold-Rolled Low-Carbon Steel

C.E. RODRÍGUEZ TORRES, F.H. SÁNCHEZ, A. GONZÁLEZ, F. ACTIS, and R. HERRERA

The suitability of the differential scanning calorimetry (DSC) technique for the quantitative study of the recrystallization process in cold-rolled steels is demonstrated, the recrystallization kinetics was described with a semiempirical model, and the transformation of a cold-rolled steel submitted to an industrial-batch thermal cycle was appropriately simulated. It was found that the activation energy for the recrystallization process depends on the heating-rate range, having values of 522 ± 13 and 259 ± 12 kJ/mole for low and high heating rates, respectively. It was concluded that the smallest value corresponds to the recrystallization process alone, while the largest one contains an additional contribution from the aluminium nitride precipitation. It is also shown that the X-ray diffraction (XRD) line-width measurement is a useful complementary method to determine the temperature regions where recovery and recrystallization occur.

I. INTRODUCTION

IT is known that metals that have been work hardened due to deformation will soften when annealed at a suitable temperature. The main process responsible for the softening is recrystallization, which involves the generation of a new grain structure of the metal. Both effects are of major technological importance for the thermomechanical processing of metallic materials.

In order to predict the course of the transformation for any given heat, it is necessary to establish the kinetics of the recrystallization process.[1,2,3] Thermal analysis methods such as differential thermal analysis (DTA) and differential scanning calorimetry (DSC) have been widely employed to determine the evolution of the transformed fraction with time (isothermal experiments) and temperature (constant-heating-rate experiments). However, these techniques have not been applied extensively to the study of recrystallization in steel. Due to the good time resolution of the calorimetric signals, it is possible to register the course of the reaction under defined experimental conditions. The process kinetics based on these data (from isothermic measurements) is usually interpreted in terms of the classic kinetic relation, developed independently by Johnson and Mehl, Avrami, and Kolmogorov (JMAK).[4,5] Unfortunately, limitations of the model frequently are overlooked. Recrystallization in many cold-worked materials does not yield linear JMAK behavior, and, in many cases, the corresponding exponents (n) fall lower than predicted.[6,7] If growth takes place isotropically in three dimensions and all nuclei are present at time zero (*i.e.*, the transformation is "site saturated"), the value of the exponent is predicted to be 3. If three-dimensional growth occurs but nuclei appear at a constant rate ("continuous nucleation"), the value of the exponent is predicted to be 4. Lower values of n are predicted for growth in less than three dimensions. In many experimental studies, however, low

values of the exponent have been found without convincing evidence for growth in less than three dimensions. This problem was reviewed by Rollett *et al.*,[8] who pointed out that the discrepancy may be caused by nonrandom distributions of the recrystallized nuclei or by a tendency of the growth rate to decrease as recrystallization proceeds. Both of these effects can be expected to arise as a result of nonuniform distribution of stored energy in the cold-worked matrix, due, for example, to the effects of grain orientation on dislocation density.

While isothermal experimental analysis techniques are, in most cases, adequate for kinetics analysis, nonisothermal thermoanalytical techniques have several advantages. The rapidity with which nonisothermal experiments can be performed makes this type of experiment attractive. Industrial processes often depend on the kinetic behavior of systems undergoing phase transformation under nonisothermal conditions. In this instance, a measurement of nonisothermal transformation kinetics is desirable.

The main purpose of the present work is to find a description of the kinetics of recrystallization, in order to predict the softening behavior of cold-worked material under different thermal conditions. The suitability of calorimetric methods for studying recrystallization processes is shown, and an alternative model based on master plots[10,11,12] of nonisothermal measurements is used. Complementary optical metallography determinations are performed in order to identify, unambiguously, the characteristic calorimetric signals. In this work, it is also shown that X-ray diffraction (XRD) is a useful complementary technique for these studies.

II. MATERIALS AND EXPERIMENTAL PROCEDURE

The low-carbon aluminum-killed steel, whose composition can be found in Table I, was produced by Siderar in the steelmaking shop. The processing route included refining in a basic-oxygen steelmaking shop, continuous casting, hot rolling on a hot strip mill, and cold rolling (to a reduction of about 67 pct after four passes) on a tandem mill. The rolled sheet (thickness of 0.82 mm) was cut with a diamond

C.E. RODRÍGUEZ TORRES, Researcher, and F.H. SÁNCHEZ, Professor, Departamento de Física, and A. GONZÁLEZ, Professor, Facultad de Ingeniera, are with the Universidad Nacional de La Plata, 1900 La Plata, and CONICET, Buenos Aires, Argentina. F. ACTIS and R. HERRERA, Researchers, are with SIDERAR, San Nicolás, Buenos Aires, Argentina.
Manuscript submitted February 27, 2001.

Table I. Chemical Composition in Mass Percent of the Employed Alloy, as Determined by Spectroscopy Emission and LECO System for the Nitrogen

C	Mn	S	P	Si	Al	Cu	N	Ni	Mo
0.0300	0.160	0.007	0.009	0.027	0.048	0.040	0.004	0.002	0.001

saw into planar sections of 3×4 mm. These were then washed in an ultrasonic cleaner.

Differential scanning calorimetry was performed on a Shimadzu DSC-50 calorimeter. Specimens with a mass of about 65 mg were annealed in platinum crucibles covered with a platinum lid. Nitrogen was used to provide a protective atmosphere (flow rate of 50 mL/min). The temperature and power axes of the instrument were calibrated from the melting endotherms of pure zinc and indium.

Continuous heating experiments were conducted at 5 °C/min, 7 °C/min, 10 °C/min, 15 °C/min, 20 °C/min, 30 °C/min, and 40 °C/min from room temperature to 700 °C. In some cases they were made at 5 °C/min and interrupted after different temperatures between 100 °C and 700 °C, in order to perform XRD and optical metallography. The XRD was performed using Cu K_α radiation with a PHILIPS* X-ray

*PHILIPS is a trademark of Philips Electronic Instruments Corp., Mahwah, NJ.

diffractometer. Methalographic examination was carried out using conventional methods. The area studied was the longitudinal cross section.

III. PRINCIPLE OF DATA PROCESSING

An alternative model, different from the conventional JMAK one, is used to describe the kinetics of the recrystallization process. It is based on the assumption that the reaction can be described by a differential equation, called the fundamental kinetic equation,

$$\frac{d\alpha}{dt} = K(T)f(\alpha) \qquad [1]$$

where $K(T)$ is a velocity constant and $f(\alpha)$ is characteristic of the solid reaction process.[9] Assuming the validity of the Arrhenius law, $K(T)$ can be expressed as

$$K(T) = k_0 \exp\left(-\frac{E_a}{RT}\right) \qquad [2]$$

where k_0 is a pre-exponential factor, E_a is the activation energy, T is the temperature, and R is the gas constant.

The $f(\alpha)$ functions can be derived on the basis of different models of the reaction interface movement, and their corresponding mathematical expressions are well known.[5] From the kinetic equation (Eq. [1]), it is possible to determine $f(\alpha)$ by measuring $d\alpha/dt$ (using DSC, for example) for a material with a known activation energy.

From the representation of the experimentally obtained $f(\alpha)$ vs α value and its comparison with those derived from different models, the most appropriate $f(\alpha)$ value and the values of the parameters of each model could be chosen.[10,11,12] The form of the $f(\alpha)$ function, corresponding to the JMAK model, is

$$f(\alpha) = n(1 - \alpha)\,(\ln\,(1 - \alpha))^{1-\frac{1}{n}} \qquad [3]$$

However, many processes not described by Eq. [3] can be better explained using a two-parameter model:[13,14]

$$f(\alpha) = \alpha^M\,(1 - \alpha)^N \qquad [4]$$

where M and N define the relative contributions of the acceleratory and decay regions of the kinetic process. It was shown that this two-parameter model is physically meaningful only for $M < 1$. This model is a plausible mathematical description for nucleation and growth in noncrystalline or highly deformed solids. It has been shown that this expression can describe any experimental $f(\alpha)$ curve, even those that fit the JMAK model. In this case, the kinetic exponents take values of $M_{Av} \cong 0.79$ and $N_{Av} \cong 0.72$ (for an Avrami exponent of $n = 4$) and $M_{Av} \cong 0.70$ and $N_{Av} \cong 0.75$ (for $n = 3$). A larger value of the kinetic exponent M indicates a more important role of the transformed phase on the overall kinetics, and $N > 1$ indicates increasing complexity. However, the intent to equate the parameters M and N with a definite crystallization mechanism should be avoided. Meaningful conclusions concerning the real mechanism of the process should be based on other types of complementary evidence.

A master plot, which is a characteristic curve independent of the measurement conditions, can be used to determine if a kinetic process is of the JMAK type or not.[15] There are two functions, $y(\alpha)$ and $z(\alpha)$, that can be easily obtained by a simple transformation of DSC data, and which, after normalizing to the (0,1) range, describe a master curve. These functions are defined as

$$z(\alpha) = \frac{1}{\beta}\frac{d\alpha}{dt}\,\pi(x)T \qquad [5]$$

$$y(\alpha) = \frac{d\alpha}{dt}\exp\left(\frac{E_a}{RT}\right) \qquad [6]$$

with $\pi(x)$ being a rational expression.[15]

These functions exhibit maxima at α_M and α_P, respectively. The latter remains constant at a value of $\alpha_P = 0.632$, for the JMAK model. Then this value can, therefore, be used as a simple test for the applicability of this model.[15,14] The validity of Eq. [1] can be verified by checking the invariance of the $y(\alpha)$ and $z(\alpha)$ plots with respect to process variables, such as heating rate, that test the isokinetic hypothesis upon which the equation is built. The activation energy (E_a) is needed in order to calculate these functions. The value of E_a can be determined by an isoconversional method,[16] without assuming the kinetic-model function. From the logarithmic form of Eq. [1], it follows that E_a is obtained from the slope of the ln $(d\alpha/dt)$ vs $1/T$ plot for a constant α value. The E_a value should be practically independent of the fractional conversion in the $0.3 \leq \alpha \leq 0.7$ range. Some changes may be expected for lower and higher values of α, because of larger relative errors in the baseline interpolation for peak tails.
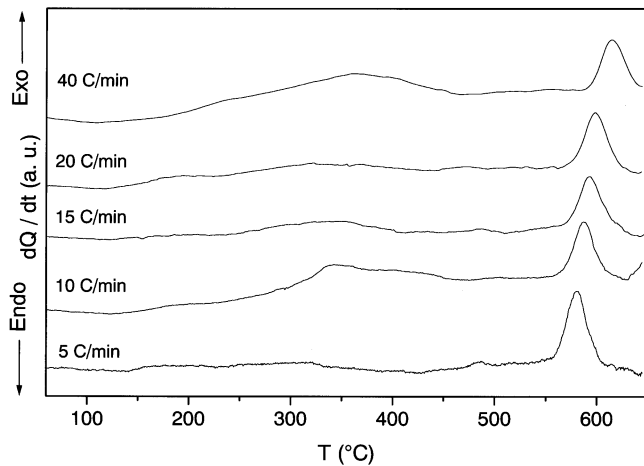
Fig. 1—Dynamic DSC curves at 5 °C/min, 10 °C/min, 15 °C/min, 20 °C/min, and 40 °C/min.

IV. RESULTS

Figure 1 represents the DSC dynamic scan obtained by continuous heating at various heating rates. It shows a well-defined exothermic peak, centered at ≈580 °C, and a broad distribution between 137 °C and 400 °C. The areas under these two regions yield transformation enthalpies of 40 and 35 J/mole, respectively. The photomicrographs in Figure 2 show the microstructures of samples rapidly cooled from annealing temperatures after heating at a rate of 5 °C/min. The inhomogeneity of deformation is evident in the nonuniform substructure in Figure 2(a) and is reflected in the presence of a number of "dark grains." Carbides that precipitated during coiling at the hot-rolling step are broken during the cold-rolling process and appear mainly at the grain boundaries aligned along the rolling direction.

At 470 °C (Figure 2(b)), no evidence of recrystallization is observed. At 530 °C (Figure 2(c)), the existence of many new grains at the borders of the original ones is evident, indicating that recrystallization has begun. Figure 2(d) (550 °C) shows the strong inhomogeneity of the recrystallization process. Large, completely recrystallized, grains coexist with regions of original (deformed) grains surrounded by small new grains. Figure 2(e) (570 °C) shows the advance of the process and a structure similar to that in Figure 2(d). The process has been completed at 590 °C (Figure 2(f)), and a wide distribution of sizes is evident. After the 600 °C treatment, the grain-size distribution becomes narrower (Figure 2(g)) and, finally, abnormal grain growth is observed at 650 °C (Figure 2(h)). Therefore, it can be concluded that the 580 °C DSC peak is due to the recrystallization reaction. The broad calorimetric signal that precedes this peak is most probably related to the recovery process. Studies to further clarify its origin will be performed.

The X-ray line broadening is a parameter related primarily to the degree of nonuniform lattice strain[17] and was used to follow the kinetics of recovery and recrystallization. This was carried out by monitoring the evolution of the line width. Peak profiles were obtained from samples prepared using an interrupted heating test. Figure 3 shows the evolution of the 220 diffraction-peak width with the interruption temperature for heating at 5 °C/min. Already at 100 °C, a line width reduction is observed, which proceeds at constant rate up

to about 530 °C, where the slope suddenly increases. For temperatures above 600 °C, the line width remains constant. This behavior is similar to that reported by Mukunthan and Hawbolt, for the evolution of another parameter related to the XRD line width in an interstitial-free steel, although this parameter could not be recorded for the initial process stages ($T < 300$ °C).[3] The stage, which occurs below 530 °C, is associated with recovery, while the second region is associated with recrystallization. This is in agreement with the optical metallography and DSC results.

V. KINETICS ANALYSIS

Figure 4 shows the recrystallization fraction (α), obtained from DSC measurements, as a function of temperature at scanning rates in the range from 5 °C/min to 40 °C/min. The value of α was obtained from the DSC measurements after subtraction of the background (Figure 5). The activation energy for the process was determined from these results by employing the isoconversional method described in Section III (Figure 6). The activation energy as a function of fractional conversion is shown in Figure 7 (open squares). This value is almost constant in the $0.3 \le \alpha \le 0.7$ range and has an average of $E_a = 336 \pm 6$ kJ/mole. It is clear that the experimental data in Figure 6 do not display the expected linear behavior. Instead, the results suggest the existence of one activation energy for the lower heating rates and another one for higher heating rates. From the fit of the data in Figure 7 with two straight lines, values of $E^l_a = 522 \pm 13$ kJ/mole and $E_a^h = 259 \pm 12$ kJ/mole are obtained for the low and high heating rates, respectively (refer to the open triangles and open circles in Figure 7). Besides recovery and recrystallization, precipitation of aluminum nitrides takes place during annealing. It has been reported[18,19] that for sufficiently low heating rates, nitride precipitation precedes recrystallization. For sufficiently high rates, the sequence is reversed. For intermediate rates, both processes interfere, and the nitride precipitation causes a strong retardation of recrystallization.[1,18] This fact could be the reason for the different activation-energy values seen at low and high heating rates.

In order to clarify the results presented in Figure 7, an annealing treatment to promote nitride precipitation was carried out at 500 °C for 1.5×10^5 s. After that, DSC experiments at different heating rates (5 °C/min, 10 °C/min, 20 °C min, and 40 °C/min) were performed and the activation energy was recalculated. Here, the ln ($d\alpha/dt$) vs $1/T$ expected linear dependence is observed (Figure 8). The obtained values for E_a are included in Figure 7 (closed triangles). A full agreement between these results and those obtained from high-heating-rate experiments on as-prepared samples can be observed. This confirms that the high value of E^l_a is due to the influence of aluminum nitride precipitation on recrystallization. Indeed, the E^h_a value (259 ± 12 kJ/mole) obtained in this work lies within the range reported for recrystallization in steels (125 to 370 kJ/mol).[1] It is higher than the value reported in the same work for a similar type of steel (157 kJ/mole), but activation energies have been found to depend on strain, the reduction degree, and material purity.[20]

Figure 9 shows the $y(\alpha)$ and $z(\alpha)$ functions for different heating rates. The similarities among the $y(\alpha)$, as well as
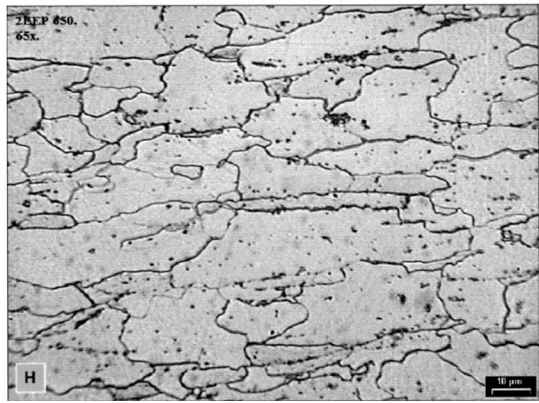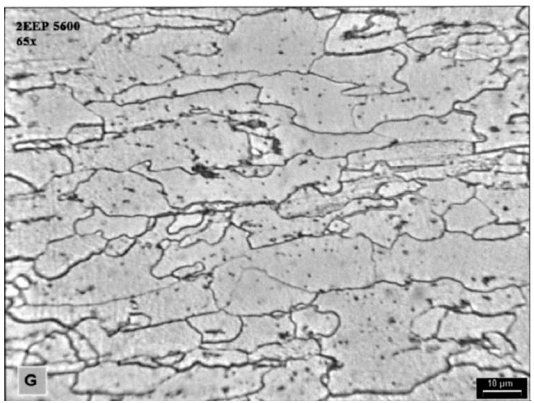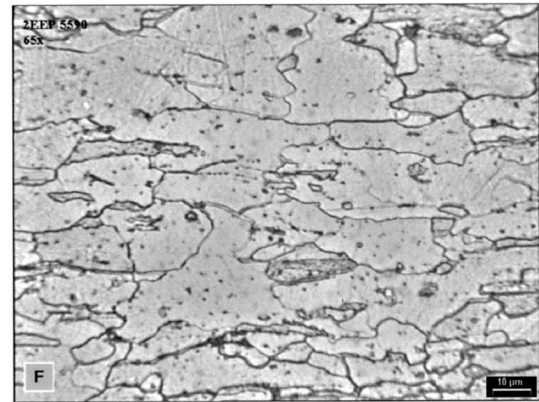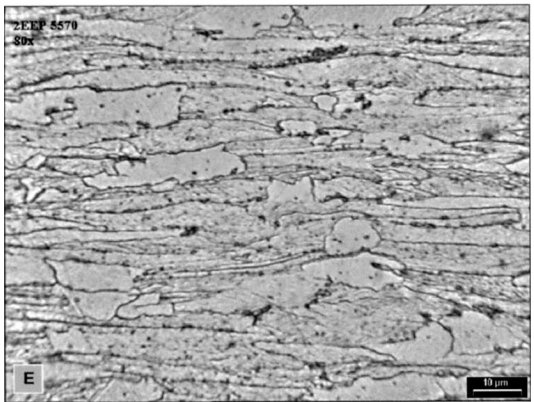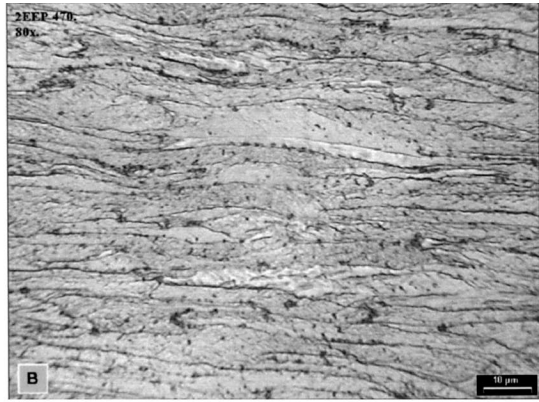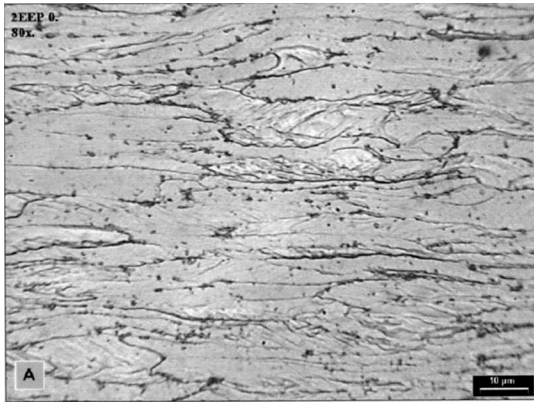
Fig. 2—Optical photomicrographs showing the microstructure evolution of the steel as prepared and under different final annealing temperatures (4 70C, 530 °C, 550 °C, 570 °C, 590 °C, 600 °C, and 650 °C) during the heating at 5 °C/min.
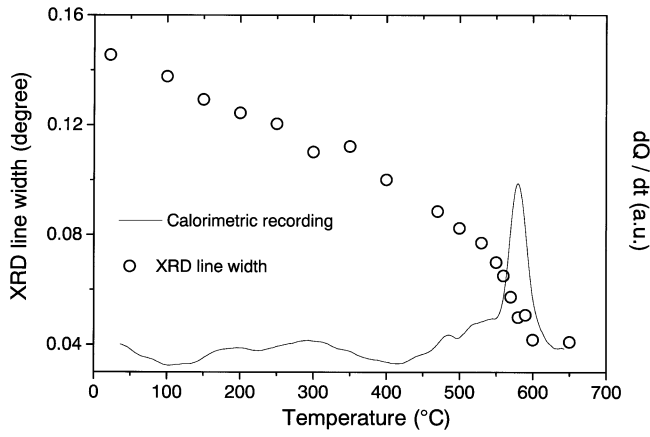
Fig. 3—Evolution of the (220) diffraction peak width with the interruption temperature for scans performed at 5 °C/min (circles). The corresponding DSC curve (straight line) is shown for comparison.
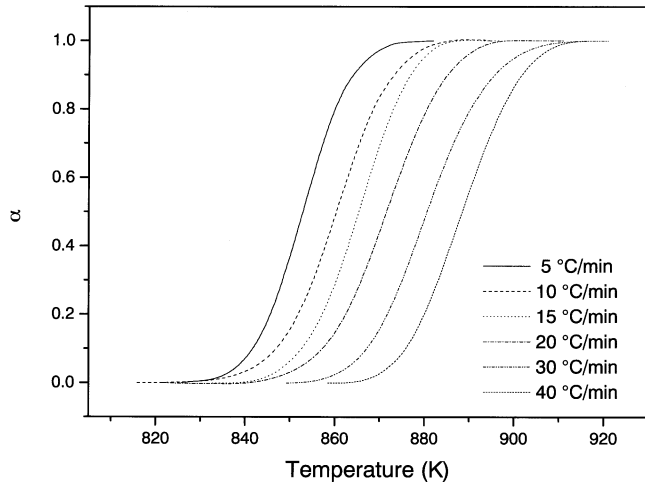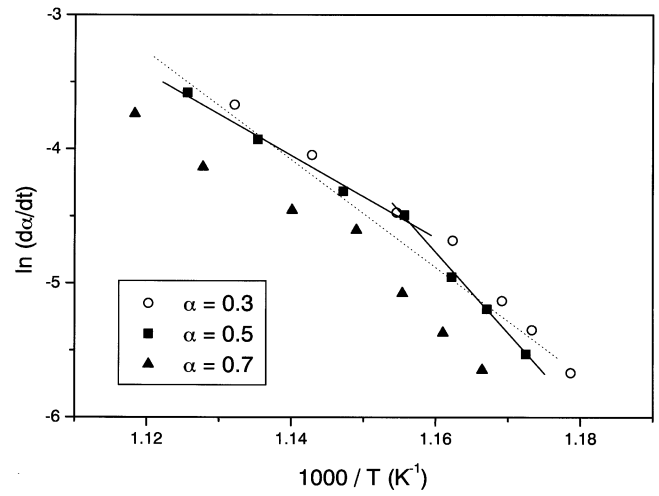

Fig. 6—Plot of ln $(d\alpha/dt)$ vs $1/T$ for different constant recrystallized fractions α. The nonlinear arrangement of data indicates the nonunique value E_a. The dotted line shows the fit for $\alpha = 0.5$ using just one activation energy, while the full lines correspond to a fit with the activation energy model.
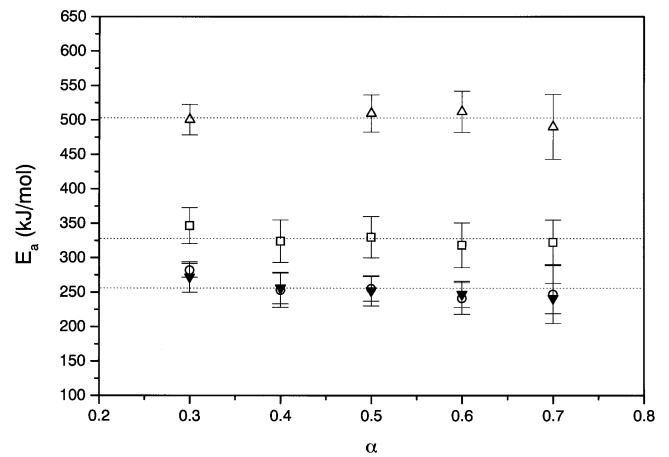

Fig. 4—Recrystallized fraction α (obtained from DSC curves) vs temperature for heating at scan rates in the range 5 °C/min to 40 °C/min.

Fig. 7—Activation energy as a function of fractional conversion α. Squares represent results obtained for the one activation energy model, while open triangles and circles represent the low and high heating rate activation energy values. Closed triangles represent E_a determined after a previous thermal annealing done in order to precipitate aluminum nitride.
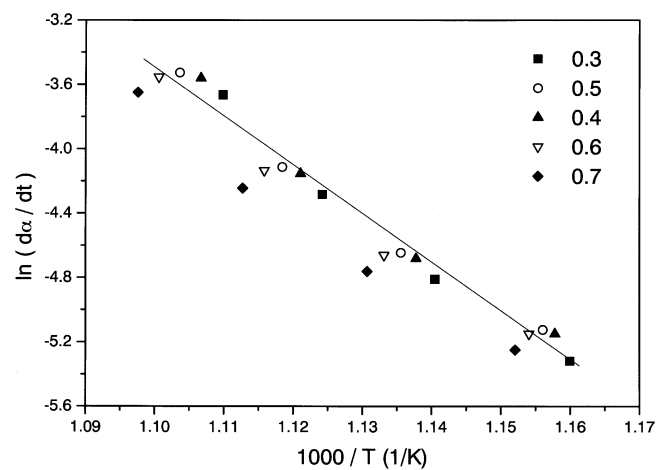

Fig. 5—Diagram showing the starting and ending points for calculation of recrystallized fraction α.

Fig. 8—Plot of ln $(d\alpha/dt)$ vs $1/T$ for different constant recrystallized fractions α, after a thermal treatment at 500 °C during 1.5×10^5 s. The straight line shows the fit for $\alpha = 0.5$ with one activation energy.
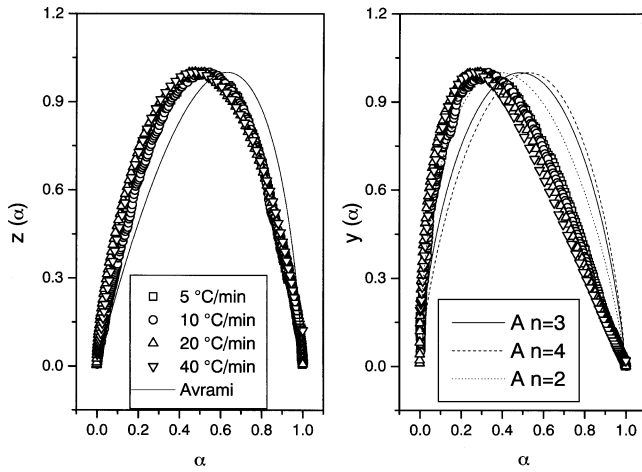
Fig. 9—Normalized $z(\alpha)$ and $y(\alpha)$ functions derived from nonisothermal DSC data for the recrystallization of cold-worked steels. For comparison, the curves corresponding to the JMAK model are included. The fit with the empirical function (Eq. [4]) cannot be distinguished from the experimental data.

Fig. 10—Dotted and full curves show simulated recrystallized fraction using the average activation energy of 336 kJ/mole and $E_a^l = 522$ kJ/mole, respectively. Squares represent Vickers hardness experimental values. All data for a typical batch thermal cycle after cold rolling.

among the $z(\alpha)$, functions indicate that the isokinetic hypothesis seem to be fulfilled. The maximum of the $z(\alpha)$ function does not fall in the range predicted for the JMAK model ($\alpha_P = 0.632$, as indicated in Section III), suggesting that this model is not valid for the recrystallization kinetics. The function used to describe $y(\alpha)$ is the empirical two-parameter model given in Eq. [6], with $M = 0.50 \pm 0.05$ and $N = 1.2 \pm 0.1$. In this $y(\alpha)$ plot, the maximum is shifted to lower values of α, compared to the ones corresponding to the Avrami model with $n = 2$, 3, or 4. The mathematical origin of this behavior can be ascribed to the particular values of the exponents M and N, which are $M < M_{Av}$ and $N > N_{Av}$ (Section III). Taking into account that M is related to the acceleratory region, its relatively small value may be interpreted as having originated in an early impingement due to spatially inhomogeneous nucleation and growth, as was observed by optical metallography. Both effects are probably due to the grain-boundary distribution and to the inhomogeneity of the initial state of deformation, as was observed for several metals and alloys.[20]

Once the activation energy E_a, the pre-exponential factor k_0, and the function $f(\alpha)$ have been experimentally determined, the transformed fraction $\alpha(t,T)$ can be obtained by integrating Eq. [1]:

$$g(\alpha) = \int_0^{\alpha} \frac{d\alpha'}{f(\alpha')} = \int k_0 e^{-\frac{E_a}{RT(t')}} dt' \qquad [7]$$

for any thermal cycle ($T(t)$). For the case in which $M = 0.5$ and $N = 1$, which are the values obtained for the lower-heating-rate scan (5 °C/min), an analytical solution can be derived:

$$\alpha(t,T) = \left(\frac{B-1}{B+1}\right)^2 \qquad [8]$$

where B is the numerical integral

$$B(t,T) = \int k_0 e^{-\frac{E_a}{RT(t')}} dt' \qquad [9]$$

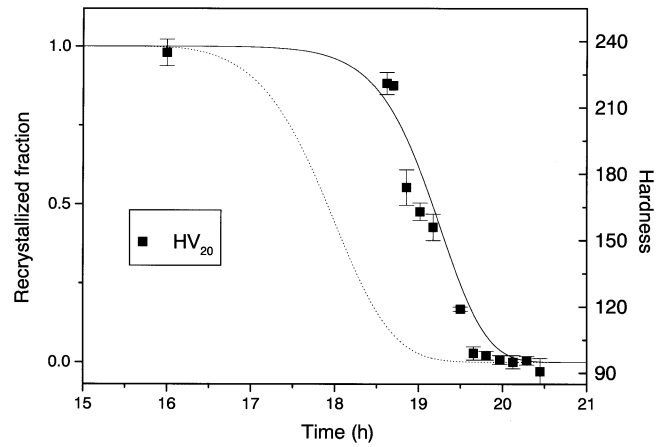The function $\alpha(t)$, simulated for a typical batch thermal cycle, *i.e.*, $\beta_1 = 30$ °C/h from room temperature to 500 °C, followed by $\beta_2 = 12.5$ °C/h from 500 °C to 600 °C, is shown in Figure 10. The full line represents the simulated function using $E_a^l = 522$ kJ/mole (low heating rates), while the dotted one is obtained with $E_a = 336$ kJ/mole (average value). Squares show the diminution of the measured hardness which is assumed to be proportional to the degree of transformation in specimens submitted to this cycle in our laboratory. The coincidence of the experimental points with the full curve is very good, indicating that E_a^l describes the data even at heating rates much lower than those used in the determination of the function $\alpha(t,T)$.

VI. CONCLUSIONS

It is shown that the DSC technique provides a weak but clear signal of the recrystallization process, which allows its quantitative study. Its advantage with respect to other techniques is that it allows a continuous monitoring of the transformed fractions, the determination of the starting and ending transformation temperatures, and an accurate estimation of the heat of transformation.

The present results indicate that the activation energy for the recrystallization process depends on the heating-rate range. Its values, obtained with the isoconversional method, are $E_a^l = 522 \pm 13$ kJ/mole and $E_a^h = 259 \pm 12$ kJ/mole for low ($\beta < 15$ °C/min) and high ($\beta > 15$ °C/min) heating rates, respectively. The term E_a^l corresponds to a physical situation where recrystallization and aluminum nitride precipitation coexist, while E_a^h corresponds solely to recrystallization. The kinetics of the process were described using the fundamental kinetic equation based on a two-parameter empirical model for $f(\alpha)$. From it, an expression for the transformed fraction for any thermal cycle was obtained. A good agreement between the transformed fraction simulated with this expression and that calculated from hardness measurements for a typical industrial-batch cycle was found.

The metallography observations show that the recrystallization is not homogeneous, but the nucleation and growth are faster in some deformed grains. The XRD linewidth determination is also a useful complementary method to

determine the temperature regions where different processes, *i.e.*, recovery and recrystallization, occur.

REFERENCES

1. W. Bleck, W. Müschenborn, and L. Meyer: *Steel Res.*, 1988, vol. 59, p. 334.
2. C. Liu, A.J.C. Burghardt, T.H. Jacobs, and J.J.F. Scheffer: *37th MWSP Conf. Proc., ISS*, 1996, vol. 33, p. 963.
3. K. Mukunthan and E.B. Hawbolt: *Metall. Mater. Trans. A*, 1996, vol. 27A, p. 3410.
4. J.W. Christian: *The Theory of Phase Transformations in Metals and Alloys*, Pergamon Press, New York, NY, 1975, [Part I].
5. F.L. Cumbrera and F. Sánchez-Bajo: *Thermochim. Acta*, 1989, vol. 14, p. 7231.
6. C.W. Price: *Acta Metall. Mater.*, 1990, vol. 38, p. 727.
7. P. Krüger and E. Woldt: *Acta Metall. Mater.*, 1992, vol. 40, p. 2933.
8. A.D. Rollett, D.J. Srolovitz, R.D. Doherty, and M.P. Anderson: *Acta Metall.*, 1989, vol. 37, p. 627.
9. J.H. Sharp and S.A. Wentworth: *Anal. Ceram. Soc.*, 1969, vol. 41, p. 2060.
10. J.M. Criado: *Thermochim. Acta*, 1978, vol. 24, p. 186.
11. J.M. Criado, J. Málek, and A. Ortega: *Thermochim. Acta*, 1989, vol. 147, p. 377.
12. J.M. Criado, A. Ortega, and F. Gotoi: *Thermochim. Acta*, 1990, vol. 157, p. 171.
13. J. Málek: *Thermochim. Acta*, 1989, vol. 138, p. 337.
14. J. Málek: *Thermochim. Acta*, 2000, vol. 355, p. 239.
15. J. Málek: *Thermochim. Acta*, 1995, vol. 267, p. 61.
16. H.L. Friedman: *J. Polymer Sci. Part C. Polymer Lett.*, 1964, vol. 6, p. 183.
17. B.D. Cullity: *Elements of X-Ray Diffraction*, 2nd ed., Addison-Wesley Publishing Co., Reading, MA, 1978, p. 281.
18. R.K. Ray, J.J. Jonas, and R.E. Hook: *Int. Mater. Rev.*, 1994, vol. 39, p. 129.
19. F.G. Wilson and T. Gladman: *Int. Mater. Rev.*, 1988, vol. 33, p. 221.
20. F.J. Humphreys and M. Hatherly: *Recrystallization and Related Annealing Phenomena*, Pergamon, Oxford, United Kingdom, pp. 195-96.